pp 1566–1577. © Royal Aeronautical Society 2016
doi: 10.1017/aer.2016.75

Coning motion stability of spinning missiles with strapdown seekers

S. He
shaoming.he.cn@gmail.com

D. Lin and J. Wang
School of Aerospace Engineering
Beijing Institute of Technology
Beijing
P.R. China

ABSTRACT

This paper investigates the problem of coning motion stability of spinning missiles equipped with strapdown seekers. During model derivation, it is found that the scaling factor error between the strapdown seeker and the onboard gyro introduces an undesired parasitic loop in the guidance system and, therefore, results in stability issues. Through stability analysis, a sufficient and necessary condition for the stability of spinning missiles with strapdown seekers is proposed analytically. Theoretical and numerical results reveal that the scaling factor error, spinning rate and navigation ratio play important roles in stable regions of the guidance system. Consequently, autopilot gains must be checked carefully to satisfy the stability conditions.

Keywords: Spinning Missile; Coning Motion Stability; Strapdown Seeker; Scaling Factor Error

Received 31 December 2015; revised 13 April 2016; accepted 14 April 2016; first published online 4 July 2016.

NOMENCLATURE

a_{cy}, a_{cz}	acceleration command
a_y, a_z	acceleration of interceptor
c	distance between onboard accelerometer and centre of gravity
F_D	drag force
F_L	lift force
I_x	longitudinal moment of inertia
I_t	lateral moment of inertia
k_a	acceleration feedback gain of three-loop autopilot
k_g	scaling factor of onboard gyro
k_p	amplifier gain of three-loop autopilot
k_r	dynamic gain of servo system under spinning
k_s	gain of servo system
k_{ss}	scaling factor of strapdown seeker
k_z	attitude angle feedback gain of three-loop autopilot
k_ω	rate feedback gain of three-loop autopilot
M_S	static moment
M_μ	Magnus moment
M_q	damping moment
M_C	control moment
N	proportional navigation gain
T_s	time constant of actuator
p, q, r	angular velocities of the non-spinning frame with respect to the inertial frame
P	propulsive force
q_z	LOS angle with respect to the inertial frame
R_d	scaling factor error
V	missile velocity
V_c	relative velocity
α	non-spinning angle-of-attack
β	non-spinning sideslip angle
δ	complex angle-of-attack
ε	angle between the LOS and the interceptor body axis
ζ	complex attitude angle
μ_s	damping ratio of actuator
ϕ_d	total delay angle
σ_{cy}, σ_{cz}	non-spinning deflection command
σ_y, σ_z	non-spinning deflection angle
ϑ, ψ, ϕ	pitch, yaw and roll angle
τ	command transmission delay of actuator

1.0 INTRODUCTION

Strapdown seekers have attracted increasing interest among engineers in recent years due to their low cost, small size and simple structure[1]. However, the strapdown seeker is fixed with missile's body and, therefore, cannot directly measure the inertial line-of-sight (LOS) rate information, which is usually required for modern guidance law implementation. To obtain

https://doi.org/10.1017/aer.2016.75 Published online by Cambridge University Press

such information, one must combine the strapdown seeker's measurement with the onboard gyro's measurement. Since the scaling factors of these two sensors are highly non-linear and non-constant, the body's attitude rate is coupled in the computation of the inertial LOS rate. As a consequence, this sensor combination inevitably induces a parasitic loop in the guidance system, which severely degrades the guidance performance and is well researched by many scholars[2-5].

Coning motion has long been used to describe the rotation of a slender body about the velocity vector, usually at high incidence due to the forces and moments arising from asymmetric vortices shed from the nosecone, as discussed in Ref. 1. This motion is usually characterised by a constant angle-of-attack. More recently, the term 'coning motion' was used in Ref. 6 to discuss the destabilising effect of yaw or Magnus moments on spinning missiles commonly at lower angles of attack. This is what we concerned with in this paper. The spinning missiles, unlike the non-spinning ones, have severe aerodynamic and control cross-couplings between the yaw channel and the pitch channel. The aerodynamic cross-couplings consist of Magnus effect and gyroscope effect caused by spinning, for which the corresponding coning motion stability was discussed in Refs 6-11. On the other hand, the control cross-couplings result from time lag of control commands transmission and actuator response[12,13]. Considering this, the stability criteria for non-spinning missiles is no longer valid for the spinning case. To solve this problem, the authors in Refs 14-17 derived analytically stable regions for spinning missiles with rate loop, attitude autopilot and acceleration autopilot. However, none of them considered spinning missiles with strapdown seekers.

Motivated by the aforementioned problem, this paper tries to propose an analytical stability condition for spinning missiles with strapdown seekers. To the best of our knowledge, this may be the first attempt in the literature. The contributions of this paper are twofold.

1) A sufficient and necessary condition for the stability of spinning missiles with strapdown seekers is proposed analytically using a complex summation method;
2) Case studies show that the parasitic loop induced by scaling factor error severely narrows the stable region and there exists a trade-off design for the navigation ratio between guidance precision and coning motion stability.

The rest of the paper is organised as follows. The model derivation is stated in Sec. 2.0. In Sec. 3.0, the stability analysis is presented in detail, followed by the numerical verifications provided in Sec. 4.0. Finally, some conclusions are offered in Sec. 5.0.

2.0 MODEL DERIVATION

2.1 Model of strapdown seeker considering scaling factor error

Taking the longitudinal plane as an example, the associated angles are defined in Fig. 1, where q_z denotes the LOS angle with respect to the inertial frame, ϑ stands for the body pitch angle with respect to the inertial frame, ε represents the angle between the LOS and the interceptor body axis. Unlike gimbal platform seeker, the strapdown seeker is fixed with missile body and, therefore, can only measure the error angle ε and its rate. Considering this, the required inertial LOS rate for the well-known proportional navigation guidance can only be obtained by combing the onboard gyro's measurement $\dot{\vartheta}$ and the strapdown seeker's measurement $\dot{\varepsilon}$.

Suppose the scaling factors of the onboard gyro and the strapdown seeker are k_g and k_{ss}, respectively. For practical strapdown seekers, the scaling factor k_{ss} is usually calibrated

https://doi.org/10.1017/aer.2016.75 Published online by Cambridge University Press

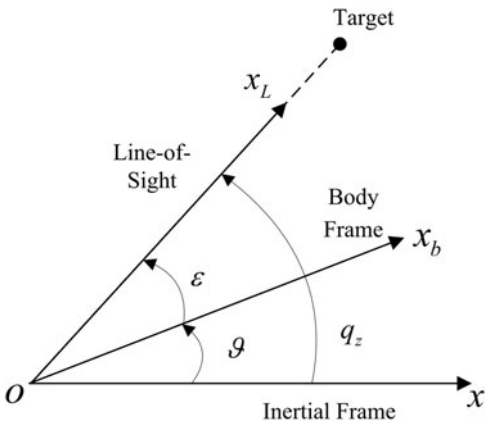

Figure 1. Model of strapdown seeker.

off-line on the ground, but it may have some unpredictable fluctuations due to environmental difference and long-term storage. Considering this, the scaling factor error always exists in real-time flight. Let $R_d = k_{ss} - k_g$ be the scaling factor error, then, the measured LOS rate can be formulated as

$$\dot{q}_z^m = \dot{q}_z + R_d \dot{\vartheta}, \qquad \ldots (1)$$

where $R_d > 0$ means positive feedback, while $R_d < 0$ denotes negative feedback.

It follows from Equation (1) that the measured LOS rate of strapdown seeker has an additional term $R_d\dot{\vartheta}$ compared with gimbal platform seeker and, therefore, results in a parasitic loop in the guidance loop.

2.2 Model of spinning missile

To establish the mathematical equations of spinning missiles, the pitch and yaw motion of spinning missiles are described in non-spinning body coordinates, where the non-spinning angle-of-attack and equivalent control effects are used. According to Ref. 18, the dynamic equations of a symmetric spinning missile can be formulated as

$$\begin{aligned}
\dot{\alpha} &= -p\beta + q - (F_L/mV)\,\alpha - [(P - F_D)/mV]\,\alpha \\
\dot{\beta} &= p\alpha - r - (F_L/mV)\,\beta - [(P - F_D)/mV]\,\beta \\
\dot{q} &= (M_S/I_t)\,\alpha - \left(M_\mu/I_t\right)\left(p + \dot{\phi}\right)\beta + \left(M_q/I_t\right) q \\
&\quad + (M_C/I_t)\,\sigma_y - (I_x/I_t - 1)\,pr - (I_x/I_t)\,\dot{\phi} r \\
\dot{r} &= (M_S/I_t)\,\beta - \left(M_\mu/I_t\right)\left(p + \dot{\phi}\right)\alpha + \left(M_q/I_t\right) r \\
&\quad + (M_C/I_t)\,\sigma_z - (I_x/I_t - 1)\,pq - (I_x/I_t)\,\dot{\phi} q,
\end{aligned} \qquad \ldots (2)$$

where F_L, P, F_D are lift force, propulsive force and drag force, respectively; M_S, M_μ, M_q and M_C are static moment, Magnus moment, damping moment and control moment, respectively; I_x and I_t are longitudinal moment of inertia and lateral moment of inertia, respectively; α, β

https://doi.org/10.1017/aer.2016.75 Published online by Cambridge University Press

are non-spinning angle-of-attack and sideslip angle, respectively; p, q, r are angular velocities of the non-spinning frame with respect to the inertial frame; $\dot{\phi}$ is the spinning rate.

By defining $q = \dot{\vartheta}$, $r = \dot{\psi}$, $a_1 = F_L/mV$, $a_2 = (P - F_D)/mV$, $b_{11} = M_S/I_t$, $b_{12} = M_\mu/I_t$, $b_{21} = I_x/I_t$, $b_{22} = M_q/I_t$, $b_3 = M_C/I_t$ and under small angle assumption, the non-linear dynamics in Equation (2) can be linearised as

$$\begin{aligned}
\dot{\alpha} &= \dot{\vartheta} - (a_1 + a_2)\,\alpha \\
\dot{\beta} &= -\dot{\psi} - (a_1 + a_2)\,\beta \\
\ddot{\vartheta} &= b_{11}\alpha + b_{12}\dot{\phi}\beta - b_{21}\dot{\phi}\dot{\psi} + b_{22}\dot{\vartheta} + b_3\sigma_y \\
\ddot{\psi} &= b_{11}\beta - b_{12}\dot{\phi}\alpha + b_{21}\dot{\phi}\dot{\vartheta} + b_{22}\dot{\psi} + b_3\sigma_z
\end{aligned} \qquad \ldots (3)$$

The onboard actuator is modelled as the following second-order system

$$\frac{\sigma}{\sigma_c} = \frac{k_s e^{-\tau s}}{T_s^2 s^2 + 2\mu_s T_s s + 1}, \qquad \ldots (4)$$

where σ_c denotes the generated command signal; $1/T_s$, μ_s, τ stand for natural frequency, damping ratio and command transmission delay, respectively. For a given constant spinning rate $\dot{\phi}$, the relationship between the input and output of the servo system in the non-spinning system can be obtained as[14]

$$\begin{bmatrix} \sigma_y \\ \sigma_z \end{bmatrix} = k_s k_r \begin{bmatrix} \cos\phi_d & \sin\phi_d \\ -\sin\phi_d & \cos\phi_d \end{bmatrix} \begin{bmatrix} \sigma_{cy} \\ \sigma_{cz} \end{bmatrix}, \qquad \ldots (5)$$

where k_s is the gain of the servo system; k_r and ϕ_d are the dynamic gain of the servo system under spinning and the total delay angle, respectively, which are governed by the following equations[14]

$$k_r = \frac{1}{\sqrt{\left(1 - T_s^2\dot{\phi}^2\right)^2 + \left(2\mu_s T_s\dot{\phi}\right)^2}} \qquad \ldots (6)$$

$$\phi_d = \arccos\left(1 - \frac{T_s^2\dot{\phi}^2}{\sqrt{\left(1 - T_s^2\dot{\phi}^2\right)^2 + \left(2\mu_s T_s\dot{\phi}\right)^2}}\right) + \tau\dot{\phi} \qquad \ldots (7)$$

2.3 Model of autopilot

Due to its robustness and effectiveness, the classical three-loop autopilot was widely accepted in modern engineering applications. This kind of autopilot consists of an angular rate feedback loop, an attitude angle feedback loop and an acceleration feedback loop. Each of these three loops has its own specific functions. The rate loop is used to increase the damping ratio of the missile and improve the transient performance. The attitude loop is used to stabilise the attitude of the missile and improve the overall performance. The acceleration loop is used to increase the tracking precision of the autopilot. The command signals for the three-loop

https://doi.org/10.1017/aer.2016.75 Published online by Cambridge University Press

autopilot are[19]

$$\begin{bmatrix} \sigma_{cy} \\ \sigma_{cz} \end{bmatrix} = \begin{bmatrix} -\int k_p \left(a_{cz} - k_a \left(a_z + c\ddot{\vartheta}\right)\right) - k_z\vartheta - k_\omega\dot{\vartheta} \\ \int k_p \left(a_{cy} - k_a \left(a_y + c\ddot{\psi}\right)\right) - k_z\psi - k_\omega\dot{\psi} \end{bmatrix}, \quad \ldots (8)$$

where k_p, k_a, k_z, k_ω are the amplifier gain, acceleration feedback gain, attitude angle feedback gain and rate feedback gain, respectively; and c denotes the distance between the onboard accelerometer and the centre of gravity. Without loss of generality, it is assumed that the accelerometer is placed at the centre of gravity, i.e. $c = 0$, and the acceleration feedback gain equals one.

For missiles using the well-known proportional navigation guidance, one has

$$\begin{bmatrix} a_{cz} \\ a_{cy} \end{bmatrix} = \begin{bmatrix} -NV_c\dot{q}_z^m \\ NV_c\dot{q}_y^m \end{bmatrix} = \begin{bmatrix} -NV_c\left(\dot{q}_z + R_d\dot{\vartheta}\right) \\ NV_c\left(\dot{q}_y + R_d\dot{\psi}\right) \end{bmatrix} \quad \ldots (9)$$

For stability analysis, it can be assumed that the system inputs $\dot{q}_z$ and $\dot{q}_y$ are zero. Then, the command signals can be further written as

$$\begin{bmatrix} \sigma_{cy} \\ \sigma_{cz} \end{bmatrix} = \begin{bmatrix} \dfrac{k_pVa_1}{a_1+a_2}\alpha - \left(\dfrac{k_pVa_1}{a_1+a_2} + k_z - NV_cR_d\right)\vartheta - k_\omega\dot{\vartheta} \\ -\dfrac{k_pVa_1}{a_1+a_2}\beta - \left(\dfrac{k_pVa_1}{a_1+a_2} + k_z - NV_cR_d\right)\psi - k_\omega\dot{\psi} \end{bmatrix} \quad \ldots (10)$$

2.4 Model of overall system

Following the above subsections, the overall system can be modelled as Fig. 2. One can see that the scaling factor error induces an additional parasitic loop in the system.

To simplify the mathematical expressions, complex summation is used to formulate the dynamics of the spinning missile. Defining the complex angle-of-attack as $\delta = -\beta + i\alpha$ and the complex attitude angle as $\zeta = \psi + i\vartheta$, then, it follows from Equation (3) that

$$\begin{aligned} \dot{\delta} &= \dot{\zeta} - (a_1 + a_2)\,\delta \\ \ddot{\zeta} &= \left(b_{11} - ib_{12}\dot{\phi}\right)\delta + \left(b_{22} - ib_{21}\dot{\phi}\right)\dot{\zeta} + b_3\left(\sigma_z + i\sigma_y\right) \end{aligned} \quad \ldots (11)$$

Similarly, defining the complex control signal as $\sigma = \sigma_z + i\sigma_y$, based on Equation (5), one has

$$\sigma = k_s k_r \left(\cos\phi_d - i\sin\phi_d\right)\left(\sigma_{cz} + i\sigma_{cy}\right) \quad \ldots (12)$$

Substituting Equation (10) into Equation (12) gives

$$\sigma = k_s k_r \left(\cos\phi_d - i\sin\phi_d\right)\left[\frac{k_pVa_1}{a_1+a_2}\delta - \left(\frac{k_pVa_1}{a_1+a_2} + k_z - NV_cR_d\right)\zeta - k_\omega\dot{\zeta}\right] \quad \ldots (13)$$

Further substituting Equation (13) into Equation (11) yields

$$\begin{aligned} \dot{\delta} &= \dot{\zeta} - (a_1 + a_2)\,\delta \\ \ddot{\zeta} &= \left[b_{11} - ib_{12}\dot{\phi} + b_3k_sk_r\left(\cos\phi_d - i\sin\phi_d\right)\frac{k_pVa_1}{a_1+a_2}\right]\delta \end{aligned}$$

https://doi.org/10.1017/aer.2016.75 Published online by Cambridge University Press

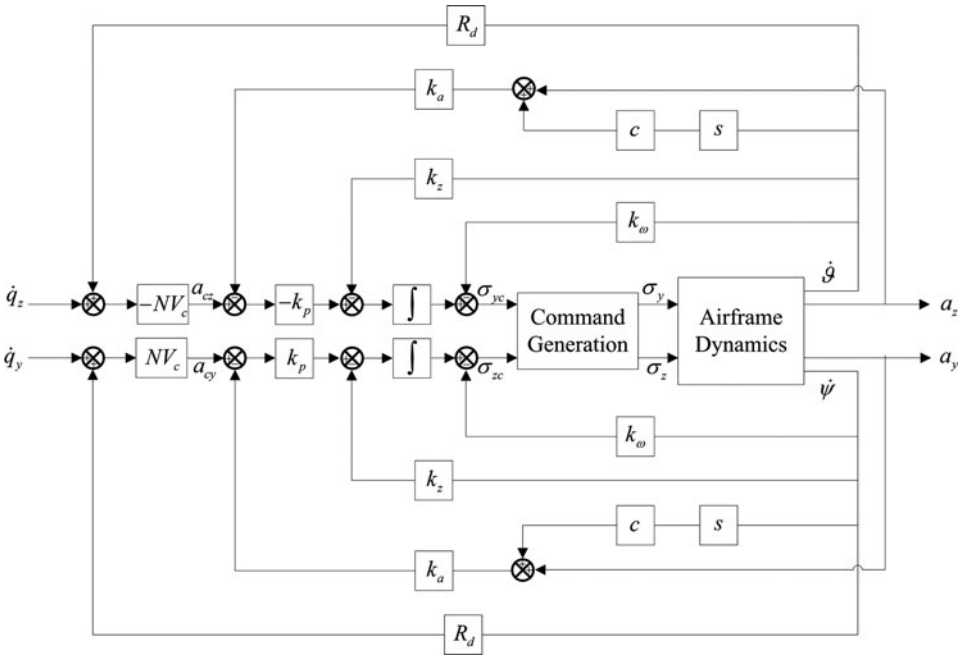

Figure 2. Model of overall system.

$$
\begin{aligned}
&- b_3 k_s k_r (\cos\phi_d - i\sin\phi_d)\left(\frac{k_p V a_1}{a_1+a_2} + k_z - NV_c R_d\right)\zeta \\
&+ \left[b_{22} - ib_{21}\dot{\phi} - b_3 k_s k_r (\cos\phi_d - i\sin\phi_d) k_\omega\right]\dot{\zeta} \qquad \ldots (14)
\end{aligned}
$$

3.0 STABILITY ANALYSIS

To analyse the stability of spinning missiles, let $x = [\ \delta \quad \dot{\zeta} \quad \ddot{\zeta}\ ]^T$ be the system state vector, and denoting $k_1 = b_3 k_s k_r$, $k_2 = b_3 k_s k_r(\cos\phi_d - i\sin\phi_d)$. Then, the closed-loop system can be formulated as

$$
\dot{x} = \underbrace{\begin{bmatrix} -(a_1+a_2) & 0 & 1 \\ 0 & 0 & 1 \\ b_{11} - ib_{12}\dot{\phi} + k_2\frac{k_p V a_1}{a_1+a_2} & -k_2\left(\frac{k_p V a_1}{a_1+a_2} + k_z - NV_c R_d\right) & b_{22} - ib_{21}\dot{\phi} - k_2 k_\omega \end{bmatrix}}_{A} x \qquad \ldots (15)
$$

The characteristic equation of the system matrix A is

$$
\begin{aligned}
&\lambda^3 + \left[(a_1+a_2) - \left(b_{22} - ib_{21}\dot{\phi} - k_2 k_\omega\right)\right]\lambda^2 + \left[-\left(b_{11} - ib_{12}\dot{\phi}\right)\right. \\
&\quad \left. - (a_1+a_2)\left(b_{22} - ib_{21}\dot{\phi}\right) + (a_1+a_2)k_2 k_\omega + k_2 k_z\right]\lambda \qquad \ldots (16) \\
&\quad + (a_1+a_2)k_2 k_z + V a_1 k_2 k_p = 0
\end{aligned}
$$

https://doi.org/10.1017/aer.2016.75 Published online by Cambridge University Press

Table 1
Simulation parameters

Parameter	Value	Parameter	Value	Parameter	Value
a_1	1.640	a_2	−0.456	b_{11}	−148.1
b_{12}	−0.151	b_{21}	0.00315	b_{22}	1.777
b_3	12.27	$V(m/s)$	1200	k_s	10
$T_s(s)$	0.016	μ_s	0.5	$\tau_s(s)$	0.009
R_d	0.05	$V_c(m/s)$	200	$\dot{\phi}$(rad/s)	8π

Rewriting Equation (16) in the format of Equation (A.1) as

$$\lambda^3 + (m_1 + in_1)\lambda^2 + (m_2 + in_2)\lambda + (m_3 + in_3) = 0, \quad \ldots(17)$$

where

$$\begin{aligned}
m_1 &= a_1 + a_2 - b_{22} + k_1 k_\omega \cos\phi_d \\
n_1 &= b_{21}\dot{\phi} - k_1 k_\omega \sin\phi_d \\
m_2 &= -(b_{11} + a_1 b_{22} + a_2 b_{22}) + [(a_1 + a_2)k_\omega + k_z]k_1 \cos\phi_d \\
n_2 &= (b_{12} + a_1 b_{21} + a_2 b_{21})\dot{\phi} + [(a_1 + a_2)k_\omega + k_z]k_1 \sin\phi_d \\
m_3 &= \left[(a_1 + a_2)k_z + V a_1 k_p\right]k_1 \cos\phi_d \\
n_3 &= -\left[(a_1 + a_2)k_z + V a_1 k_p\right]k_1 \sin\phi_d
\end{aligned} \quad \ldots(18)$$

According to Lemma 1 in Appendix A, the sufficient and necessary stability condition of spinning missiles is obtained as

$$\begin{aligned}
&m_1 > 0 \\
&m_1^2 m_2 - m_1 m_3 + m_1 n_1 n_2 - n_2^2 > 0 \\
&\left(m_1^2 m_2 - m_1 m_3 + m_1 n_1 n_2 - n_2^2\right)\left(m_1 m_2 m_3 - m_3^2 + m_1 n_2 n_3\right) \\
&\quad - \left(m_1^2 n_3 - m_1 m_3 n_1 + m_3 n_2\right)^2 > 0
\end{aligned} \quad \ldots(19)$$

The above inequality reveals that the design parameters k_ω, k_z, k_p, N and the scaling factor error R_d must satisfy certain conditions to guarantee the stability of the spinning missiles. To this end, autopilot gains must be checked carefully to satisfy the stability condition during initial designs. Although inequality (19) is relatively complex, the stable region can be easily solved by using Maple solver.

4.0 NUMERICAL VERIFICATION

In this section, the correctness of the proposed stability condition is verified by numerical simulations. The required simulation parameters are summarised in Table 1.

Without loss of generality, the navigation ratio is set as $N = 3$, and the autopilot parameters are chosen as $k_\omega = 0.7$, $k_z = 50$. By solving Inequality (19), the stable region is calculated as $k_p < 0.803$. Numerical simulations for stable, critical state and unstable coning motions with a 4° initial angle-of-attack disturbance are provided in Figs. 3, 4 and 5, respectively. The first column is $\alpha - \beta$ phase plane, while the second column is acceleration response. From these

https://doi.org/10.1017/aer.2016.75 Published online by Cambridge University Press

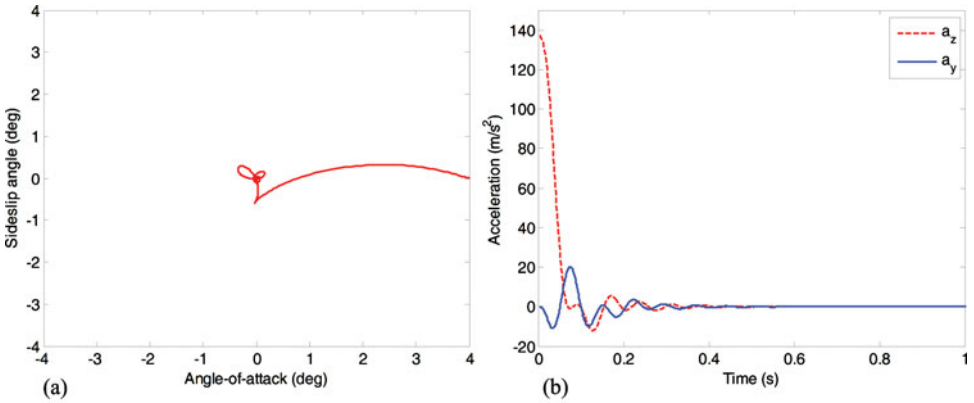

Figure 3. (Colour online) Stable coning motion with $k_p = 0.5$.

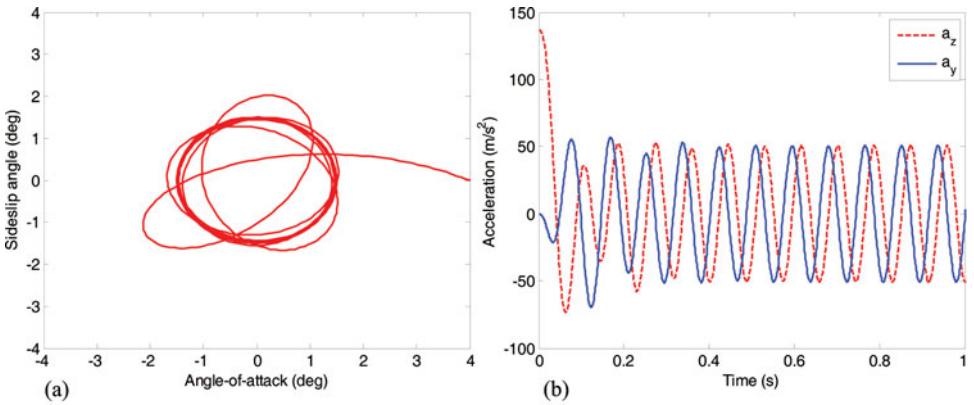

Figure 4. (Colour online) Critical state of coning motion with $k_p = 0.803$.

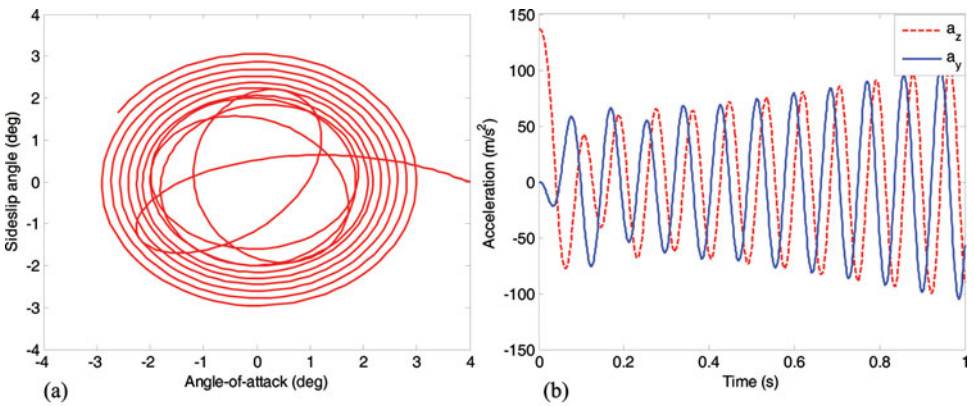

Figure 5. (Colour online) Unstable coning motion with $k_p = 0.82$.

https://doi.org/10.1017/aer.2016.75 Published online by Cambridge University Press

Table 2
Maximum values of k_p for stability under different conditions

	Spinning rate				Spinning rate		
Parameter	**4rad/s**	**6rad/s**	**8rad/s**	**Parameter**	**4rad/s**	**6rad/s**	**8rad/s**
$k_\omega = 0.6$	0.785	0.704	0.456	$k_z = 50$	0.895	0.858	0.803
$k_\omega = 0.7$	0.895	0.858	0.803	$k_z = 60$	1.044	0.981	0.833
$k_\omega = 0.8$	0.978	0.972	0.951	$k_z = 70$	1.192	1.085	0.749
$R_d = 0.03$	1.091	1.002	0.834	$N = 3$	0.895	0.858	0.803
$R_d = 0.05$	0.895	0.858	0.803	$N = 4$	0.771	0.746	0.739
$R_d = 0.07$	0.751	0.738	0.726	$N = 5$	0.678	0.673	0.672

three figures, one can note that k_p inside the stable region leads to rapid convergence to the equilibrium, k_p on the stable boundary results in a limit cycle state, and k_p beyond the stable region causes a divergent coning motion. These results, evidently, verify the correctness of the proposed analytical stability condition.

To further investigate the influence of design parameters on stable regions, the maximum values of k_p for stability under different conditions are summarised in Table 2, where the default values of the parameters, not specified in Table 2, are the same as those used in simulations for Figs. 2-5. It follows from Table 2 that the higher the spinning rate is, the smaller the upper limit of k_p becomes. For a high spinning rate, Table 2 also shows that one can increase the value of k_ω or k_z to obtain a larger stable region. Moreover, the larger the scaling factor error or navigation ratio is, the narrower the stable region is. Interestingly, in the presence of large scaling factor error or navigation ratio (see the last line in Table 2), the spinning rate plays a minor influence on the stable regions. This phenomenon also reveals that the parasitic loop induced by scaling factor error severely narrows the stable region and there exists a trade-off design for the navigation ratio between guidance precision and coning motion stability.

5.0 CONCLUSIONS

A sufficient and necessary condition of coning motion stability for spinning missiles with strapdown seekers is derived analytically and verified using numerical simulations. The results reveal that the parasitic loop induced by scaling factor error, navigation ratio and spinning rate play important roles in the stable region and, therefore, the autopilot gains must be carefully checked using the proposed criteria during the design process to satisfy the stability condition. Future work will consider real-time identification of scaling factor error and dynamic decoupling method to increase the stable region under certain conditions.

ACKNOWLEDGEMENTS

This work was supported by the National Natural Science Foundation of China (Grant No. 61172182).

https://doi.org/10.1017/aer.2016.75 Published online by Cambridge University Press

APPENDIX A. STABILITY CRITERIA OF COMPLEX COEFFICIENT SYSTEM

This section collects a useful lemma regarding the stability of a complex coefficient system, which plays a key role in stability analysis of the closed-loop guidance system.

Lemma 1. [16,17] *Consider the following complex coefficient polynomial*

$$\lambda^3 + (p_1 + iq_1)\lambda^2 + (p_2 + iq_2)\lambda + (p_3 + iq_3) = 0 \qquad \ldots (A.1)$$

The sufficient and necessary condition for all the roots of Equation (A.1) in the left-half of the complex plane is that the three inequalities $c_0 > 0$, $c_1 > 0$ and $c_2 > 0$ are satisfied simultaneously, where

$$\begin{aligned} c_0 &= p_1 \\ c_1 &= \left(p_1^2 p_2 - p_1 p_3 + p_1 q_1 q_2 - q_2^2\right)/c_0^3 \\ c_2 &= \left[\left(p_1^2 p_2 - p_1 p_3 + p_1 q_1 q_2 - q_2^2\right)\left(p_1 p_2 p_3 - p_3^2 + p_1 q_2 q_3\right)\right. \\ &\quad \left. - \left(p_1^2 q_3 - p_1 p_3 q_1 + p_3 q_2\right)^2\right]/\left(c_0^6 c_1^3\right) \end{aligned} \qquad \ldots (A.2)$$

Proof. *Readers can refer to*[16,17] *for details.*

REFERENCES

1. PARK, B.G., KIM, T.H. and TAHK, M.J. Optimal impact angle control guidance law considering the seeker's field-of-view limits, *Proceedings of the Institution of Mechanical Engineers, Part G: Journal of Aerospace Engineering*, 2013, **227**(8), pp 1347-1364.
2. KIM, D., RYOO, C.K., KIM, Y. and KIM, J. Guidance and control for missiles with a strapdown seeker, *Proceedings of International Conference on Control, Automation and Systems (ICCAS)*, 2011, Gyeonggi-do, Korea, pp 969-972.
3. WILLMAN, W.W. Effects of strapdown seeker scale-factor uncertainty on optimal guidance, *J Guidance, Control, and Dynamics*, 1988, **11**(3), pp 199-206.
4. JANG, S.A., RYOO, C.K., CHOI, K. and TAHK, M.J. Guidance algorithms for tactical missiles with strapdown seeker, *Proceedings of SICE Annual Conference, the University Electro-Communications*, 2008, Japan, pp 2616-2619.
5. YUN, J., RYOO, C.K. and SONG, T.L. Strapdown sensors and seeker based guidance filter design, *Proceedings of International Conference on Control, Automation and Systems (ICCAS)*, 2008, Seoul, Korea, pp 468-472.
6. KUHN, G.D., NIELSEN, J.N. and SPANGLER, S.B. Theoretical study of vortex shedding from bodies of revolution undergoing coning motion, NASA Contractor Report, Nielson Engineering and Research Inc., Report number NEAR TR-14, 1969.
7. PLATUS, D.H. Missile and spacecraft coning instabilities, *J Guidance, Control, and Dynamics*, 1994, **17**(5), pp 1011-1018.
8. MURPHY, C.H. Symmetric missile dynamic instabilities, *J Guidance, Control, and Dynamics*, 1981, **4**(5), pp 464-471.
9. LIAÑO, G. and MOROTE, J. Roll-rate stability limits of unguided rockets with wraparound fins, *J Spacecraft and Rockets*, 2006, **43**(4), pp 757-761.
10. PECHIER, M., GUILLEN, P. and CAYZAC, R. Magnus effect over finned projectiles, *J Spacecraft and Rockets*, 2001, **38**(4), pp 542-549.
11. MAO, X., YANG, S. and XU, Y. Coning motion stability of wrap around fin rockets, *Science in China Series E: Technological Sciences*, 2007, **50**(3), pp 343-350.
12. ZHOU, W., YANG, S. and DONG, J. Coning motion instability of spinning missiles induced by hinge moment, *Aerospace Science and Technology*, 2013, **30**(1), pp 239-245.

https://doi.org/10.1017/aer.2016.75 Published online by Cambridge University Press

13. Koohmaskan, Y., Arvan, M.R., Vali, A.R. and Behazin, F. Dynamic stability conditions for a rolling flight vehicle applying continuous actuator, *Aerospace Science and Technology*, 2015, **42**, pp 451-458.
14. Yan, X., Yang, S. and Zhang, C. Coning motion of spinning missiles induced by the rate loop, *J Guidance, Control, and Dynamics*, 2010, **33**(5), pp 1490-1499.
15. Yan, X., Yang, S. and Xiong, F. Stability limits of spinning missiles with attitude autopilot, *J Guidance, Control, and Dynamics*, 2011, **34**(1), 278-283.
16. Li, K., Yang, S. and Zhao, L. Stability of spinning missiles with an acceleration autopilot, *J Guidance, Control, and Dynamics*, 2012, **35**(3), 774-786.
17. Li, K., Yang, S. and Zhao, L. Three-loop autopilot of spinning missiles, *Proceedings of the Institution of Mechanical Engineers, Part G: J of Aerospace Engineering*, 2014, **228**(7), pp 1195-1201.
18. Zipfel, P.H. *Modeling and Simulation of Aerospace Vehicle Dynamics*, 2nd ed., American Institute of Aeronautics and Astronautics, 2007, Reston, Virginia, US.
19. Zarchan, P. *Tactical and Strategic Missile Guidance*, 5th ed., American Institute of Aeronautics and Astronautics, 2007, Reston, Virginia, US.

https://doi.org/10.1017/aer.2016.75 Published online by Cambridge University Press